Electronic Supplementary Material (ESI) for CrystEngComm.

Molecular motions of a tetraphenylethylene-derived AIEgen directly monitored through in situ variable temperature single crystal X-ray diffraction

Lian Zhou [a], Wei Meng [a], Lin Sun [b], Lin Du [c,*], Xiaopeng Xuan [d,*], Jun Zhang [a,e,*]

[a.] State Key Laboratory of Plateau Ecology and Agriculture, New Energy Photovoltaic Industry Research Center, Qinghai University, Xining 810016, P. R. China

[b.] Henan Key Laboratory of Polyoxometalate Chemistry, Institute of Molecular and Crystal Engineering, College of Chemistry and Chemical Engineering, Henan University, Kaifeng, Henan 475004, P. R. China.

[c.] Key Laboratory of Medicinal Chemistry for Natural Resource Education Ministry, Yunnan University, Kunming 650091, P. R. China.

[d.] School of Chemistry and Chemical Engineering, Key Laboratory of Green Chemical Media and Reactions, Ministry of Education, Collaborative Innovation Center of Henan Province for Green Manufacturing of Fine Chemicals, Henan Normal University, Xinxiang, Henan 453007, P. R. China.

[e.] School of Materials and Chemical Engineering, Anhui Jianzhu University, Hefei 230601, P. R. China

1. Synthesis

Both 1-bromo-1,2,2-triphenylethene (2 g, 6 mmol), 3-(tert-butoxycarbonylamino) benzeneboronic acid (1.7 g, 7.15 mmol), tetrabutylammonium bromide (80 mg, 0.25 mmol) and tetrakis(triphenylphosphine)palladium (15 mg, 0.013 mmol) are commercially available, and they were dissolved in 15 mL degassed tetrahydrofuran in a 50 mL two-neck flask. Subsequently, 4 mL potassium carbonate solution (2M) was added. This reaction mixture was heated up to 65 °C and stirred under N_2 for 20 hours , then cooled down to room temperature and concentrated by evaporation. The residue was poured into 20 mL potassium carbonate solution (2M) and filtered, and the filter residue was purified *via* silica gel flash chromatography (ethyl acetate-petroleum ether = 1:7 *v*/*v*). The product of tert-butyl (3-(1,2,2-triphenylvinyl)phenyl)carbamate (BTPC) was obtained as a white solid. Yield: 81%. ^{1}H NMR ($CDCl_3$): δ 7.37 (1 H, *s*), 7.21–7.07 (9 H, *m*), 7.06–6.90 (7 H, *m*), 6.76 (1 H, *s*), 6.71 (1 H, *d*, J = 7.6 Hz), 6.24 (1 H, *s*), 1.46 (9 H, *s*). HRMS (EI–MS) m/z found 448.2204 $[M+1]^+$, $C_{31}H_{29}NO_2$ requires 448.2200.

2. Crystallization

Pure BTPC (10 mg) was dissolved in 6 mL acetonitrile using a 10 mL glass tube by heating to about 60 ºC, then the mixture was cooled to room temperature and silently placed. After the slow volatilization of acetonitrile, the colourless rod-like crystals appeared, and one crystal was selected for single crystal X-ray diffraction determination. In the typical structures at 150 K, both the phenyl rings of C20-C25 and C26-C31 are disordered over two positions with site occupancy ration of 0.51:0.49 and 0.59:0.41, respectively.

3. Refinement

As a representative, crystal data, data collection and structure refinement detail at 150 K are given in Table S1. The structure of BTPC was solved by dual space algorithm [1] and refined by full matrix least square on F^2 [2]. All the non-hydrogen atoms were refined anisotropically, and all the H atoms were located in their ideal positions by geometrical calculation with C–H = 0.95 (phenyl) or 0.98 Å (methyl), and N–H = 0.88 Å, and refined isotropically by a riding model with U_{iso} (H) = 1.5 U_{eq} (C, methyl) or 1.2 U_{eq} otherwise. Other crystal and refinement parameters at various temperatures, from 150 to 298 K with an interval of 15 K, are given in the corresponding cif files, freely available *via* www.ccdc.cam.ac.uk/data_request/cif. The CCDC reference numbers of BTPC at different temperature were 1945384 (150 K), 2120987 (165 K), 2120988 (180 K), 2120989 (195 K), 2120990 (210K), 2120991 (225 K), 2120992 (240 K), 2120993 (255 K), 2120994 (270 K), 2120995 (285 K), 2120996 (298 K), respectively.

4. Theoretical calculation

In order to obtain the local minima structures, potential energy scans by respectively changing the C17−C19−C18−C19 and C18−C19−C26−C31 dihedral

angles from 0 to 180 º with a step of 10 º were studied. This calculation was performed with the Gaussian 09 program using Becke's three-parameter hybrid functional with the correlation functional of Lee, Yang, and Parr (B3LYP) method at 6-31+G* basis set. The B3LYP functional was selected because the previous studies have shown that this method yielded reliable results for the large molecules. The minima structures were further optimized at B3LYP/ 6-311+G** level and verified by frequency calculation, confirming the obtained geometry was the energy-optimized.

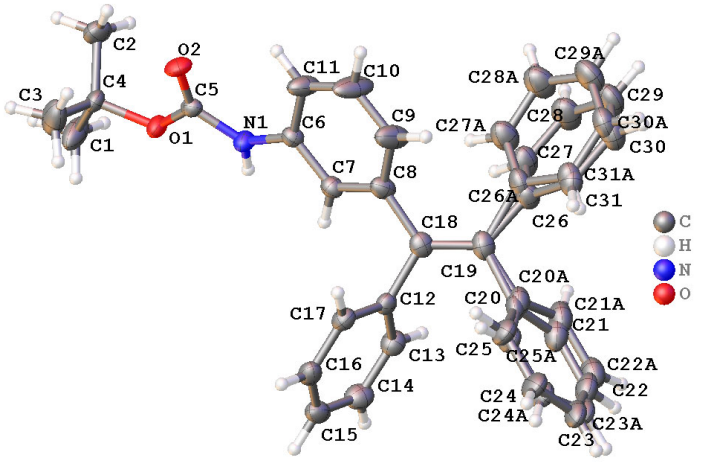

Figure S1. Asymmetric unit of BTPC with 50 % probability level at 150 K.

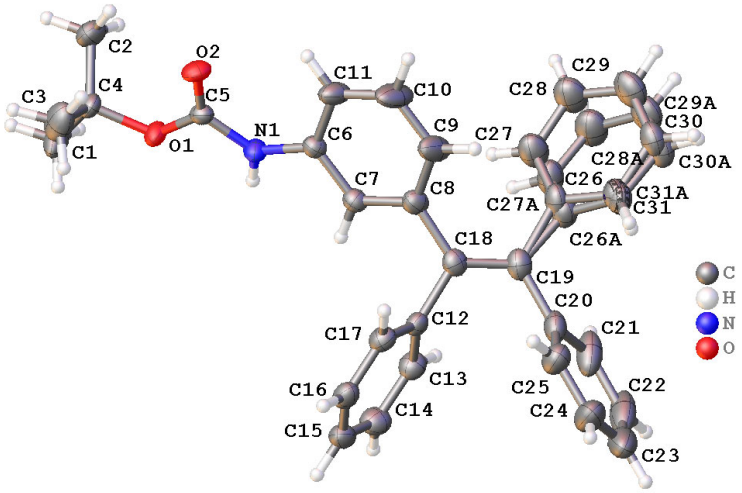

Figure S2. Asymmetric unit of BTPC with 50 % probability level at 165 K.

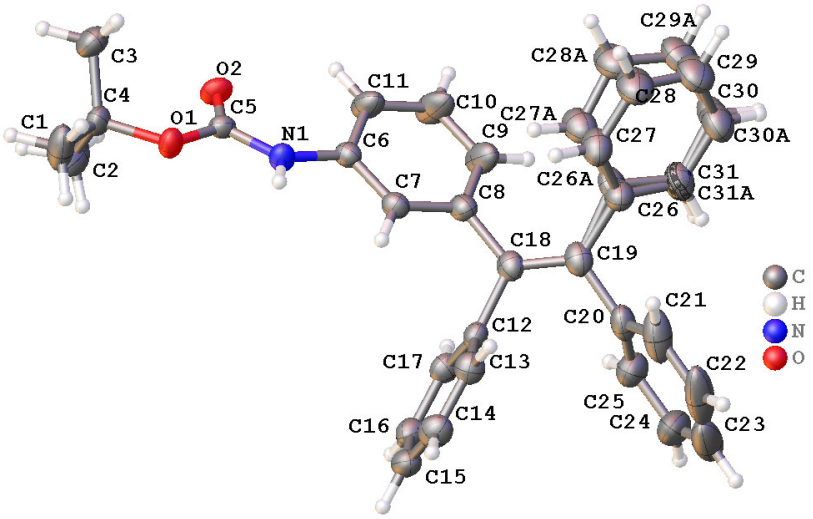

Figure S3. Asymmetric unit of BTPC with 50 % probability level at 180 K.

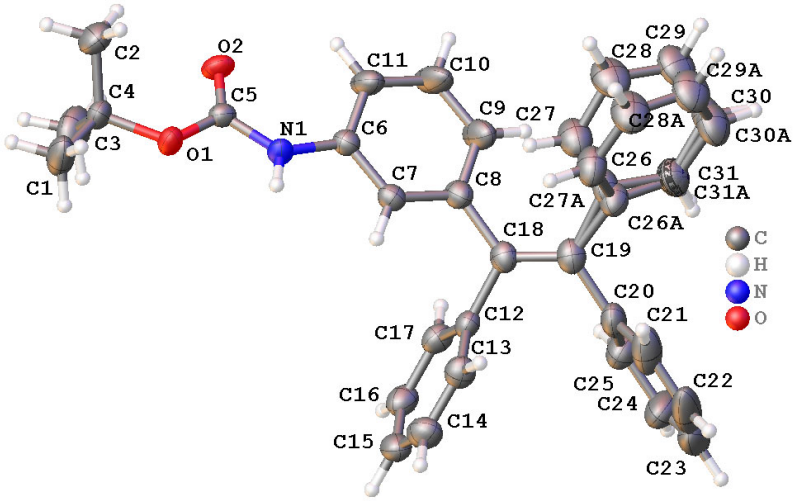

Figure S4. Asymmetric unit of BTPC with 50 % probability level at 195 K.

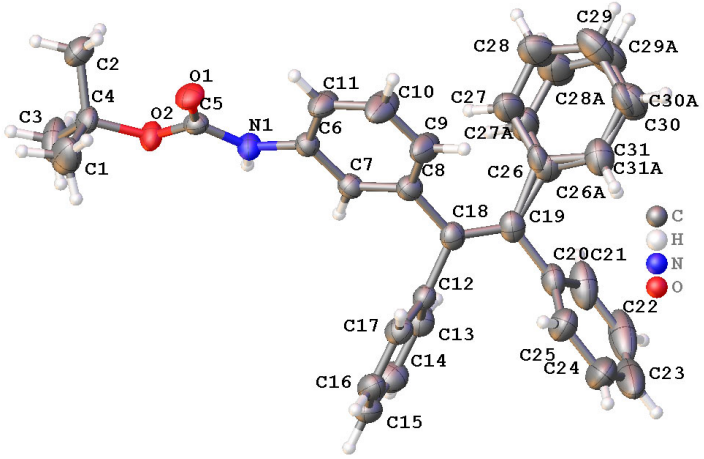

Figure S5. Asymmetric unit of BTPC with 50 % probability level at 210 K.

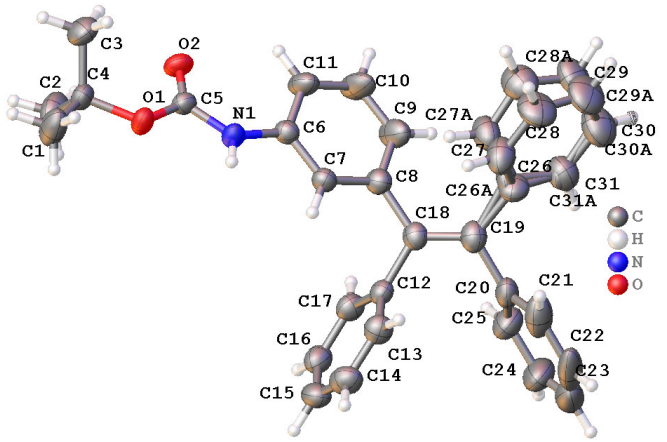

Figure S6. Asymmetric unit of BTPC with 50 % probability level at 225 K.

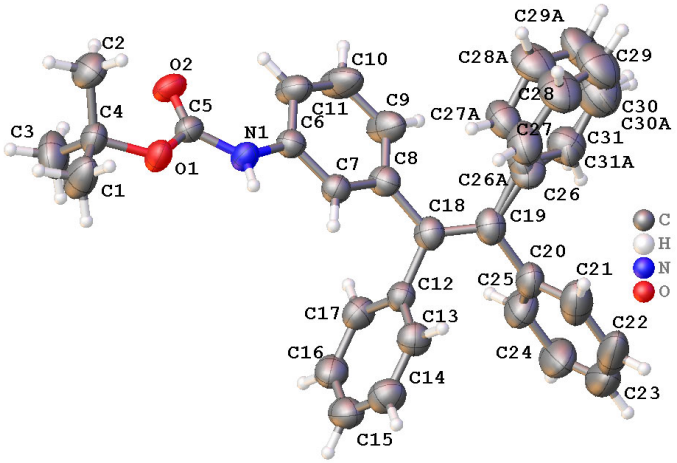

Figure S7. Asymmetric unit of BTPC with 50 % probability level at 240 K.

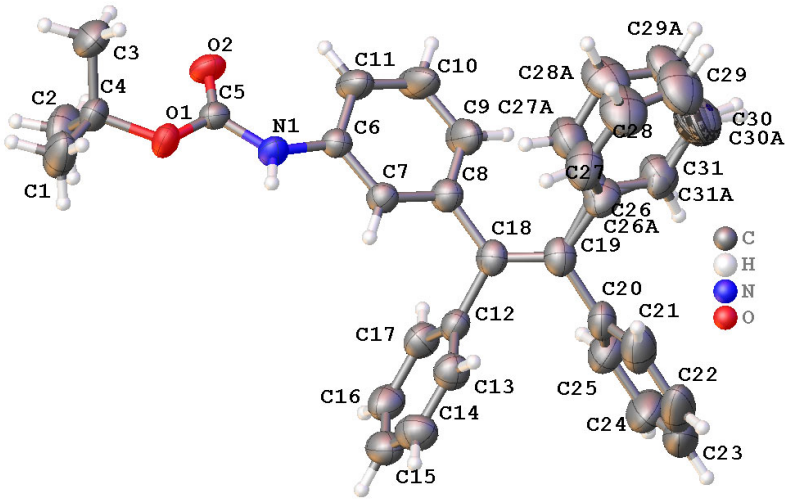

Figure S8. Asymmetric unit of BTPC with 50 % probability level at 255 K.

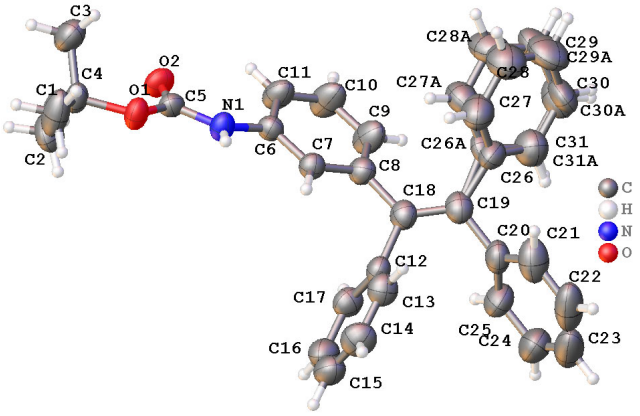

Figure S9. Asymmetric unit of BTPC with 50 % probability level at 270 K.

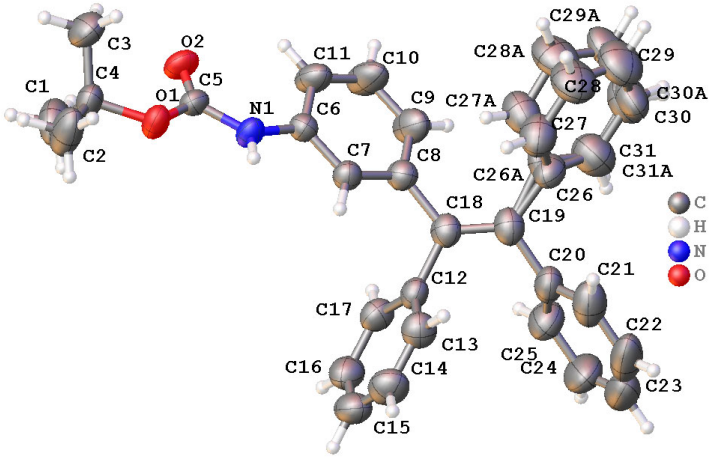

Figure S10. Asymmetric unit of BTPC with 50 % probability level at 285 K.

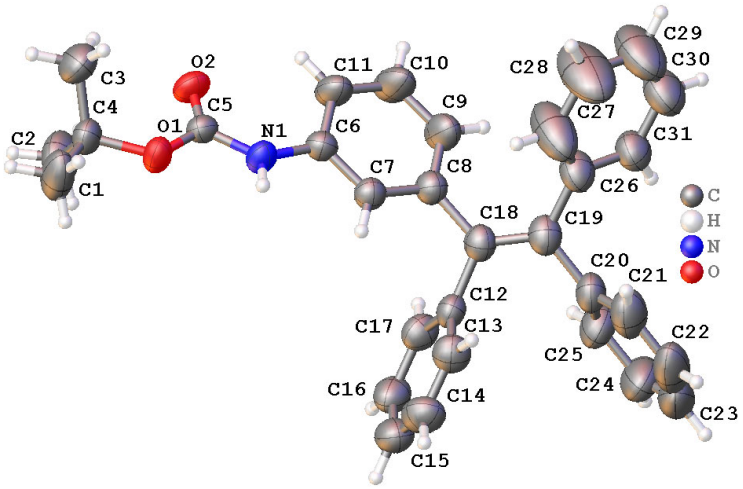

Figure S11. Asymmetric unit of BTPC with 50 % probability level at 298 K.

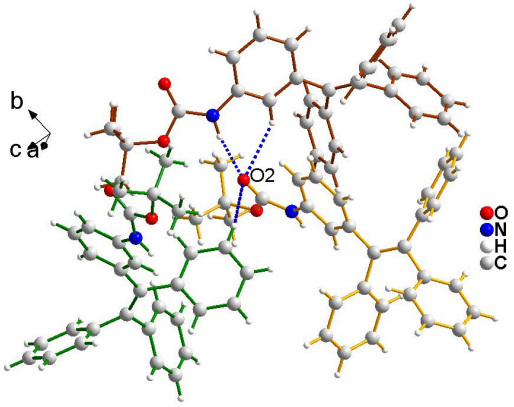

Figure S12. The intermolecular hydrogen bond interactions of BTPC

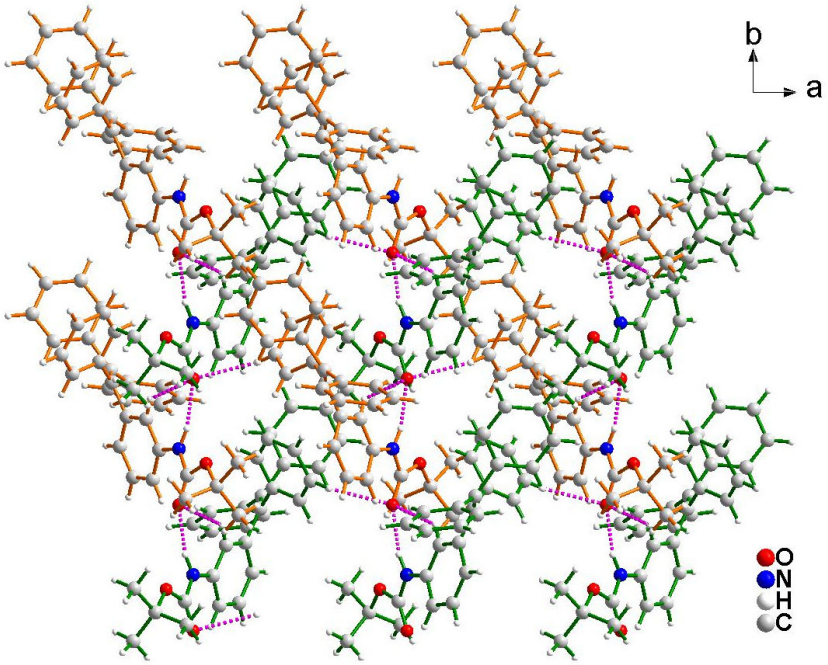

Figure S13. The 2D layer structure of BTPC.

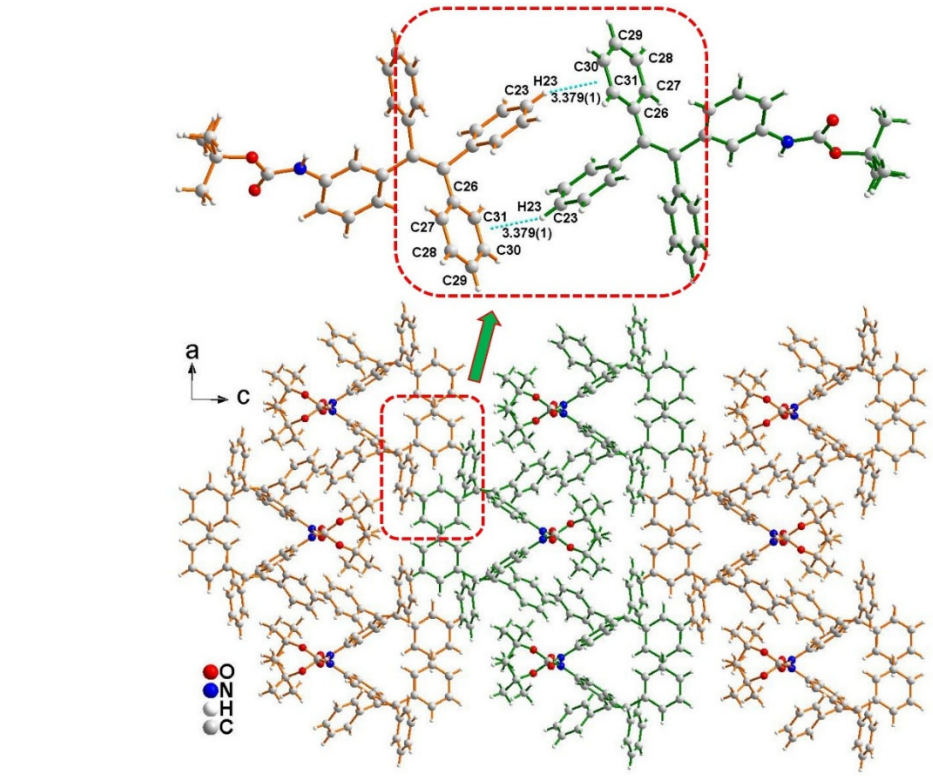

Figure S14. The 3D network of BTPC.

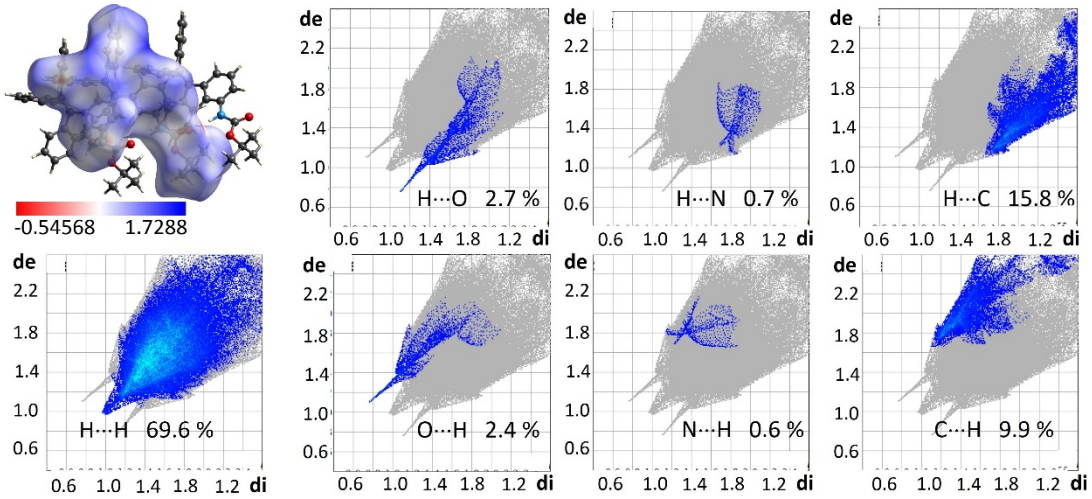

Figure S15. Hirshfeld surface and fingerprint plot for BTPC.

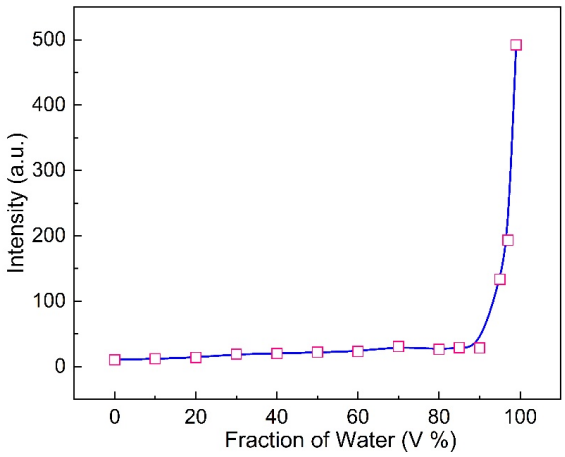

Figure S16. The variation of emission intensity for BTPC at λ_{em}=458 nm (λ_{ex}=287 nm) at different fraction of water with respect to THF.

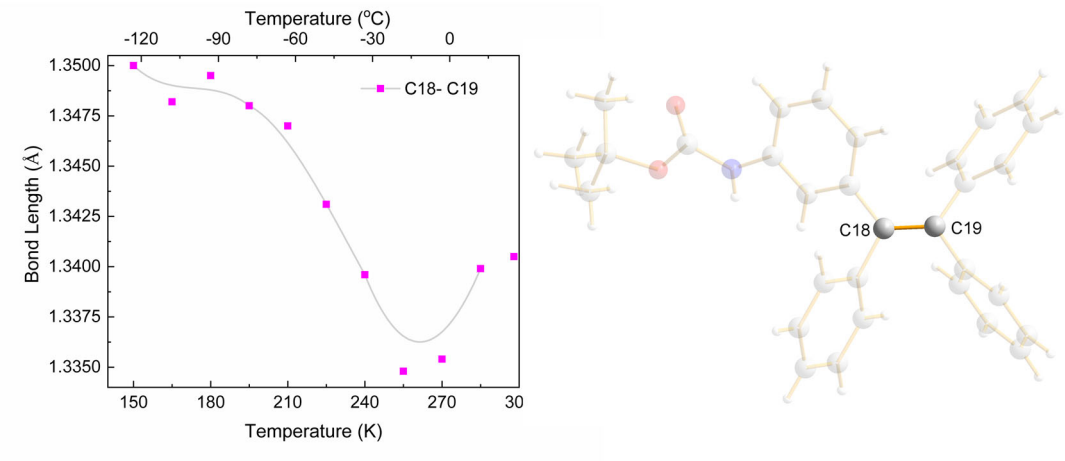

Figure S17. The change of central double bond length (C18=C19) at the different temperature.

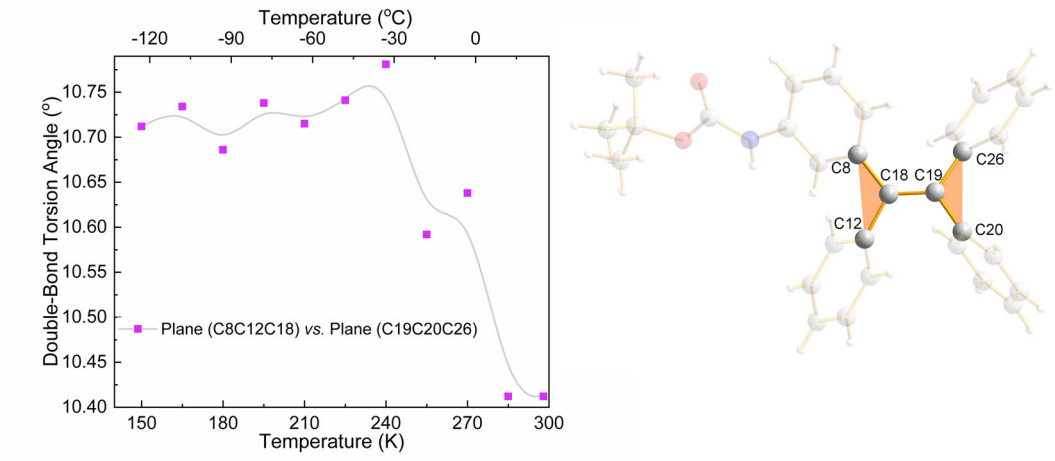

Figure S18. The change of central double bond torsion angle (C8C12C18∠C19C20C26) at the different temperature.

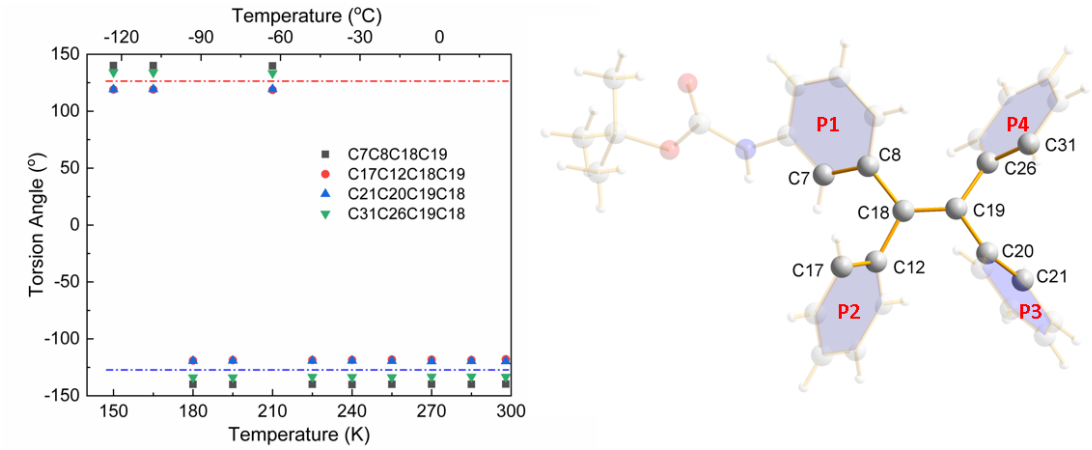

Figure S19. The change of torsion angle for the phenyls at the different temperature..

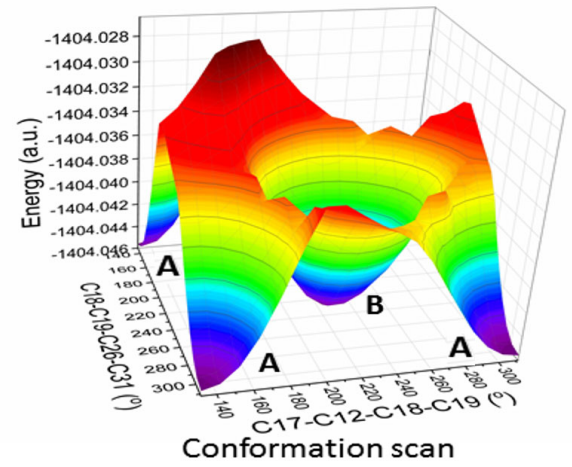

Figure S20. Potential energy scans relating to the two dihedral angles and the corresponding energy-optimized geometries (A and B). Three structures labeled by A are identical.

Table S1 Crystal data, data collection and structure refinement details at 150 K.

Item	Data
Crystal data	
Chemical formula	$C_{31}H_{29}NO_2$
M_r	447.55
Crystal system, space group	Orthorhombic, *Pbca*
Temperature (K)	150
a, *b*, *c* (Å)	16.7440 (5), 9.8734 (3), 30.618 (1)
V (Å^3)	5061.7 (3)
Z	8
Radiation type	Mo *K*α
μ (mm^{-1})	0.07
Crystal size (mm)	0.16 × 0.11 × 0.11
Data collection	
Diffractometer	Bruker *SMART APEX2* area detector
Absorption correction	Multi-scan
T_{min}, T_{max}	0.459, 0.492
No. of measured, independent and	59116, 5813, 4865
R_{int}	0.065
$(\sin \theta/\lambda)_{max}$ (Å^{-1})	0.651
Refinement	
Refinement on	F^2
$R[F^2 > 2\sigma(F^2)]$, $wR(F^2)$, S	0.084, 0.186, 1.16
No. of reflections	5813
No. of parameters	372
No. of restraints	582
H-atom treatment	H-atom parameters constrained
	$w = 1/[\sigma^2(F_o^2) + (0.0048P)^2 + 10.7033P]$
$(\Delta/\sigma)_{max}$	< 0.001
$\Delta\rho_{max}$, $\Delta\rho_{min}$ (e Å^{-3})	0.42, −0.35

Table S2 Selected hydrogen-bond parameters of BTPC at 150 K.

D—H···*A*	*D*—H (Å)	H···*A* (Å)	*D*···*A* (Å)	*D*—H···*A* (°)
N1—H1···O2^{i}	0.88	2.01(5)	2.875 (7)	165.8 (4)
C7—H7···O2^{i}	0.95	2.55(5)	3.319 (9)	137.7 (4)
C16—H16···O2^{ii}	0.95	2.57(1)	3.43 (1)	150.4 (5)

Symmetry code(s): (i) −*x*+1/2, *y*−1/2, *z*; (ii) −*x*+1, *y*−1/2, −*z*+3/2.

References:

1. Sheldrick, G. M., SHELXT - integrated space-group and crystal-structure determination. *Acta Crystallogr. A Found. Crystallogr.* **2015,** *71*, 3-8.
2. Sheldrick, G. M., Crystal structure refinement with SHELXL. *Acta Crystallogr. C Struct. Chem.* **2015,** *71*, 3-8.
3. Frisch, M.J., Trucks, G.W. , Schlegel, H.B. et al. Gaussian 09, Revision D.01 Gaussian, Inc, Wallingford CT (2013)